THE JOURNAL OF BIOLOGICAL CHEMISTRY
Vol. 274, No. 37, Issue of September 10, pp. 26240–26248, 1999
Printed in U.S.A.

Shuttling of CTP:Phosphocholine Cytidylyltransferase between the Nucleus and Endoplasmic Reticulum Accompanies the Wave of Phosphatidylcholine Synthesis during the $G_0 \rightarrow G_1$ Transition*

(Received for publication, April 22, 1999, and in revised form, June 2, 1999)

Ingrid C. Northwood, Amy H. Y. Tong‡, Bryan Crawford, Adrienne E. Drobnies, and Rosemary B. Cornell§

From the Institute of Molecular Biology and Biochemistry and the Biochemistry Program, Simon Fraser University, Burnaby, British Columbia V5A 1S6, Canada

The transition from quiescence (G_0) into the cell division cycle is marked by accelerated phospholipid turnover. We examined the rates of phosphatidylcholine (PC) synthesis and the activity, membrane affinity, and intracellular localization of the rate-limiting enzyme in the synthesis of PC, CTP:phosphocholine cytidylyltransferase (CT) during this transition. The addition of serum to quiescent IIC9 fibroblasts resulted in a wave of PC synthesis beginning at ~10 min, peaking at ~3 h with a >10-fold increase in rate, and declining to near basal rates by 10 h. CT activity, monitored *in situ*, was elevated ~3-fold between 1 and 2 h postserum. Neither CT mass nor its phosphorylation state changed during the surge in PC synthesis and CT activity. On the other hand, the ratio of particulate/soluble CT surged and then receded in concert with the wave of PC synthesis. During quiescence, CT was confined to the nucleus, as assessed by indirect immunofluorescence. Within 10 min after serum stimulation, a portion of the CT fluorescence appeared in the cytoplasm, where it intensified until ~4 h postserum. Thereafter, the cytoplasmic CT signal waned, while the nuclear signal increased, and by 8 h CT was once again predominantly nuclear. The dynamics of CT's apparent translocation in and out of the nucleus paralleled the wave of PC synthesis and the solubility changes of CT. Cytoplasmic CT co-localized with BiP, a resident endoplasmic reticulum protein, in a double labeling experiment. These data suggest that the wave of PC synthesis that accompanies the $G_0 \rightarrow G_1$ transition is regulated by the coordinated changes in CT activity, membrane affinity, and intracellular distribution. We describe for the first time a redistribution of CT from the nucleus to the ER that correlates with an activation of the enzyme. We propose that this movement is required for the stimulation of PC synthesis during entry into the cell cycle.

The regulation of phospholipid synthesis during the cell cycle is an important, yet understudied, problem. Phospholipid synthesis is required, not only to double the membrane mass, but also to replace phospholipid degraded by phospholipases. There are data suggesting regulated and periodic fluctuation of phospholipid synthesis and turnover rates during the cell cycle (1). For example, in BAC1.2F5 macrophage cells, phosphatidylcholine (PC)[1] turnover rates were high during G_1 and low during S (2).

PC is typically the major phospholipid of animal cells, and is a precursor to the synthesis of three other phospholipids: phosphatidylethanolamine, sphingomyelin, and phosphatidylserine. There is evidence that cell cycle progression may be sensitive to membrane PC content. Choline deprivation of WI-38 fibroblasts, L6 myoblasts, or C3H/10T½ fibroblasts led to decreased PC synthesis and mass and arrest in G_1 (3, 4). The addition of choline (or lyso-PC, which is rapidly acylated to form PC) restored PC content and progression into S phase. Delipidated serum on its own did not effectively restore cell cycling (4). These results suggest that serum growth factors cannot substitute for choline in the re-establishment of the cell cycle following choline starvation and that PC rather than another choline metabolite is the regulating molecule. The timing of the addition of choline during G_1 to allow normal entry into S phase suggested a requirement for PC late in G_1 (4). Chinese hamster ovary cells harboring a temperature-sensitive CT do not synthesize PC at 40 °C, and the cells accumulate in G_1. If not rescued by the addition of PC or lyso-PC, the cells undergo apoptosis rather than allowing DNA synthesis to occur (5). Induction of apoptosis in HeLa cells by the CT inhibitor, edelfosine, was prevented by overexpression of CT or by lyso-PC (6). G_1 arrest and induction of apoptosis in A549 cells by farnesol and geranylgeraniol, which act as competitive inhibitors of the final enzyme in the PC synthesis pathway, can be prevented by PC (7). Together, these studies suggest the possibility that the membrane PC content could relay to a cell cycle check point late in G_1.

What regulates the synthesis of PC during the cell cycle? Under most conditions, the rate-limiting and regulated step in PC synthesis is the formation of CDP-choline, catalyzed by CTP:phosphocholine cytidylyltransferase (CT). CT is regulated post-translationally by reversible association with membrane lipids, which are required for its activity (8–11). The equilibrium between soluble and membrane-bound forms is influenced by the lipid composition of the target membrane and by the phosphorylation state of the enzyme. Phosphorylation on multiple C-terminal sites stabilizes the soluble form of the enzyme (12–14). The lipid second messengers phosphatidic acid

* Funded by Canadian Medical Research Council Grant 12930 (to R. B. C.) and a grant from the Natural Sciences and Engineering Research Council (to B. P. Brandhorst). The costs of publication of this article were defrayed in part by the payment of page charges. This article must therefore be hereby marked "*advertisement*" in accordance with 18 U.S.C. Section 1734 solely to indicate this fact.

‡ Present address: Dept. of Biology, Queens University, Kingston, Ontario K7L-3N6, Canada.

§ To whom correspondence should be addressed. Tel.: 604-291-3709; Fax: 604-291-5583; E-mail: cornell@sfu.ca.

[1] The abbreviations used are: PC, phosphatidylcholine; CPT, choline phosphotransferase; CT, CTP:phosphocholine cytidylyltransferase; DAG, diacylglycerol; FBS, fetal bovine serum; ER, endoplasmic reticulum; MEM, minimal essential medium; DMEM, Dulbecco's modified Eagle's medium; BSA, bovine serum albumin; PBS, phosphate-buffered saline.

and diacylglycerol promote CT-membrane binding (14, 15). Pretranslational regulation of CT has also been observed in response to growth factors (16, 17) and during lung development (18). In Bac1.2F5 cells, CT activity, assayed in cell extracts, was high in middle to late G_1, declined during S, and reached a minimum in G_2 (2). This pattern in activity was paralleled by changes in the enzyme's phosphorylation state. Activity was lowest when the level of phosphorylation was highest (2). The membrane interactions of the enzyme were not examined in this study.

Using *in situ* methods, CT has been localized to the nucleus in some cells, the cytoplasm in others, and to both sites in still others (19, 20). Biochemical fractionations of cells have yielded CT in the cytosol, nuclear, ER, and even Golgi fractions (21–23). CT contains a functional nuclear localization signal near its N terminus (24). Deletion of this signal resulted in mostly cytoplasmic rather than nuclear localization when expressed in the Chinese hamster ovary cells lacking endogenous CT, but disruption of the nuclear localization did not perturb cell growth or PC synthesis (24). These results suggest that nuclear localization of CT is not required for PC synthesis. Since other enzymes of phospholipid synthesis are ER residents, including cholinephosphotransferase, the enzyme catalyzing the step subsequent to the CT step, the ER localization makes functional sense. However, the role of the enzyme in the nucleus remains a mystery.

The focus of the present work is on the changes in PC synthesis and CT activity and intracellular localization during progression from the quiescent G_0 stage into the cell division cycle. Growth factors that release cells from G_0 stimulate PC turnover and the production of lipid second messengers at early steps (1, 25, 26). Growth factors also stimulate PC synthesis (16, 27–31), perhaps as a homeostatic response to the rapid acceleration of PC degradation (8, 32, 33). The stimulation of PC synthesis by serum in 3T3 cells involved an acceleration at both the choline kinase and CT steps (28), whereas angiotensin (31) and fetal pneumocyte factor (30) stimulated only CT. Our studies have employed IIC9 fibroblasts. The kinetics of lipid second messenger production in response to growth factors have been carefully dissected in IIC9 cells (25, 34, 35), making them ideal for analysis of the coupling between phospholipid degradation and synthesis during exit from G_0. We show that exit from G_0 is accompanied by a wave of PC synthesis that is coordinated with CT activation, CT translocation to membranes, and redistribution from the nucleus to the ER. The data give rise to the novel hypothesis that it is the ER-associated and not the nuclear form of CT that is enzymatically active with respect to PC synthesis.

MATERIALS AND METHODS

Antibodies—Monoclonal anti-Grp78 (BiP) was purchased from StressGen. Anti-cyclin D-1 (H-295) and purified cyclin D-1 protein (amino acids 1–295) were purchased from Santa Cruz Biotechnologies, Inc. (Santa Cruz, CA). Generation of anti-M (rabbit polyclonal antibody directed against a peptide corresponding to amino acids 256–288 of rat liver CT) has been previously described (36). Antibody to CT-β was a generous gift from Dr. Suzanne Jackowski (St. Judes Children's Research Hospital, Memphis, TN). Oregon Green and Texas Red-conjugated antibodies, rhodamine hexyl ester, and rhodamine phalloidin were all purchased from Molecular Probes, Inc. (Eugene, OR). Horseradish peroxidase-conjugated goat anti-rabbit antibody was from Sigma.

Cell Culture and Serum Starvation—IIC9 cells (a generous gift from Dr. D. Raben, Johns Hopkins, Baltimore, MD) were maintained in α-MEM/F-12 (1:1), 10% FBS, 100 units/ml penicillin, and 100 μg/ml streptomycin (Life Technologies, Inc.) as described (34) and were used at passage numbers 30–40. To generate quiescent cells, cultures (80% confluent) were washed twice with serum-free α-MEM/F12 and incubated for 48 h in starvation medium containing DMEM, 100 units/ml penicillin, 100 μg/ml streptomycin, 1 mM L-glutamine (Life Technologies, Inc.), 1 mg/ml radioimmunoassay grade BSA (Sigma), 20 mM Hepes, pH 7.4 (Sigma), and 5 μg/ml human transferrin (Calbiochem). Nonadherent cells were removed at ~30 h by aspiration, and fresh serum starvation medium was replaced. For each analysis described below, following serum starvation for 48 h, FBS was added to one set of cultures to a final concentration of 10%. The control set was maintained on serum starvation medium.

[^{3}H]Thymidine Incorporation into DNA—To measure DNA synthesis rates, [^{3}H]thymidine (NEN Life Science Products) was added to duplicate 30-mm dishes to a concentration of 2 μCi/ml in a volume of 2 ml. After 2 h at 37 °C, the medium was removed, and the dishes were washed three times with ice-cold PBS, twice with ice-cold 5% trichloroacetic acid, and once with ice-cold ethanol. The acid-insoluble material was solubilized with 0.2% SDS in 0.1 N NaOH, and the label was quantitated by liquid scintillation counting.

[^{3}H]Choline Incorporation into PC—Duplicate 60-mm dishes were labeled for 10 min at 37 °C with 10 μCi of [*methyl*-^{3}H]choline (Amersham Pharmacia Biotech) in 3 ml of medium. Incorporation of label was quenched by removing the medium, washing three times with ice-cold buffer A (50 mM Tris-HCl, pH 7.4, 0.15 M NaCl, 1 mM EDTA), and extracting into methanol. The ^{3}H incorporated into PC was analyzed in the $CHCl_3$ fraction of a Bligh-Dyer extraction (37). To measure choline transport into the cells, triplicate dishes were pulsed for 5 min with 10 μCi of [^{3}H]choline in 3 ml of medium. Incorporation of label was quenched as above. The cells were scraped from the dish into methanol and sonicated. Radioactivity was quantitated by liquid scintillation counting.

PC Mass—Duplicate 100-mm dishes were washed three times with buffer A, and cells were released from the dishes with buffer A containing 2.5 mM EDTA and counted with a hemocytometer. The lipids were extracted into $CHCl_3$ by the method of Bligh-Dyer (37). The $CHCl_3$ fraction was dried under N_2 and dissolved in 30 μl of $CHCl_3$. PC was separated from the other lipids by TLC on Silica Gel G (Analtech) using $CHCl_3$/MeOH/NH_4OH (65:35:5). The PC was visualized by I_2 staining and quantitated using the Bartlett assay (38). Egg PC (Avanti) was used as a standard.

[^{3}H]Phosphocholine and CDP-choline Turnover—IIC9 cells were labeled with 2 μCi/ml [^{3}H]choline in DMEM (28 μM choline) per 60-mm dish during the final hour of serum starvation. This labeling time was sufficient to saturate the aqueous choline metabolites in the serum-starved cells. Cultures were chased with fresh, unlabeled DMEM containing 250 μM choline with or without 10% FBS. At times after chase, the medium was aspirated, and dishes were washed three times with ice-cold PBS and quenched with 1.4 ml of MeOH. The cells were scraped into the methanol, and the aqueous phase of a Bligh-Dyer extraction was obtained. Choline (3.75 μmol), phosphocholine (4.2 μmol), and CDP-choline (0.46 μmol) were added as carriers to the samples, followed by evaporation to dryness in a Speed Vac. The residue was redissolved in 130 μl of water, and the choline metabolites were separated as described (39).

Digitonin Permeabilization—Digitonin permeabilization was carried out in a 3 °C room. Duplicate 100-mm dishes were rinsed with ice-cold PBS and placed on a Bellco rocker platform. 1.3 ml of permeabilization buffer (10 mM Hepes, pH 7.4, 0.1 M KCl, 2 mM dithiothreitol, 0.5 mM phenylmethylsulfonyl fluoride, 0.2 mg/ml digitonin (Calbiochem)) was added to each dish. At intervals thereafter, the medium was collected, and the cell ghosts were scraped in 1.2 ml of permeabilization buffer. Both fractions were transferred to tubes containing 25 μl of 5 mM PC/oleic acid (1:1) vesicles to stabilize the CT. The ghost fraction was sonicated for 20 s on ice, and aliquots were removed immediately from both fractions for assay of CT activity (40).

^{35}S Labeling of CT—100-mm dishes were grown to subconfluence, washed twice in cysteine- and methionine-free DMEM (Life Technologies, Inc.), and starved for 30 min in the same medium. The cells were then incubated with cysteine- and methionine-free DMEM supplemented with 50 μCi/ml [^{35}S]methionine and cysteine (Amersham Pharmacia Biotech) and 5% FBS. After 4 h, the cells were washed twice with ice-cold PBS and 1 ml of immunoprecipitation buffer was added to each plate. Immunoprecipitation of cell extracts was carried out as described below.

Immunoprecipitation and Immunoblotting—150-mm dishes were washed twice with PBS, and the cells were scraped into 1 ml of immunoprecipitation buffer (PBS containing 50 mM Tris pH 8.0, 1 mM EDTA, 1 mM phenylmethylsulfonyl fluoride, 1% Triton X-100, 1 mM dithiothreitol). The cells were homogenized by freeze-thaw followed by five passages through a 27-gauge needle. Insoluble material was removed by centrifugation at 14,000 $\times$ *g* for 15 min, and the supernatant was incubated with 2 μl/ml of rabbit polyclonal anti-M overnight at 4 °C. 40

μl of protein A beads (Amersham Pharmacia Biotech) were added, and the sample was incubated for 1 h at 4 °C. The protein A beads were washed four times with immunoprecipitation buffer, 40 μl of Laemmli buffer was added to the washed beads, and the samples were boiled for 5 min. Immunoprecipitated CT was resolved on a 12% SDS-polyacrylamide gel. For Western blots, proteins were transferred from 12% gels to a polyvinylidene difluoride membrane (Bio-Rad) at 150 mA for 1 h. The transfer buffer consisted of 39 mM glycine, 48 mM Tris, 20% methanol, 0.0375% SDS. Immunoblots were blocked in PBS containing 6% powdered milk, 0.5% Tween 20 and probed with anti-M (1:1000) for 1 h at room temperature. Following three washes with PBS containing 0.5% Tween 20, blots were incubated with horseradish peroxidase-conjugated goat anti-rabbit secondary antibody (1:2000) for 1 h. The blots were washed three times with PBS-Tween, and CT was visualized using enhanced chemiluminescence (Amersham Pharmacia Biotech). Detection of cyclin D1 followed a similar protocol, using an anti-cyclin D1 antibody at a dilution of 1:500.

^{32}P Labeling of CT—IIC9 cells were grown to 80% confluence in 100-mm dishes and serum-starved as described above for 32 h. Dishes were then washed twice with phosphate-free DMEM and incubated for 16 h with the same medium containing [^{32}P]orthophosphate (0.1 mCi/ml). This labeling time was sufficient to saturate the ATP pools and the ^{32}P label in CT. FBS or BSA was added to the dishes to final concentrations of 10 or 5%, respectively, and the incubation was continued. At various times, the medium was removed, and the cells were washed twice with ice-cold PBS and lysed as described above using 1 ml of immunoprecipitation buffer containing 60 mM β-glycerophosphate and 50 mM Na_3VO_4. Lysates were immunoprecipitated and resolved as described above. ^{32}P-Labeled CT was detected by autoradiography.

Immunofluorescence Microscopy—IIC9 cells were grown on coverslips to 80% confluence and serum-starved as described above. Cells were fixed in 2% paraformaldehyde-PBS for 20 min and permeabilized by incubation in PBS containing 0.5% Triton X-100, 5% BSA for 1 h at room temperature. The fixed, permeabilized cells were incubated with primary antibodies (1:100) in PBS containing 0.5% Triton X-100, 5% BSA for 2 h at room temperature or overnight at 4 °C. The cells were then washed three times with PBS and incubated with secondary antibody (1:200) for 2 h at room temperature, washed three times with PBS, and mounted in Prolong antifade reagent (Molecular Probes). For double labeling, the primary antibodies and their corresponding secondary antibodies were incubated sequentially. Cells were viewed with a Zeiss LSM-410 confocal microscope equipped with a krypton/argon laser (Omnichrome), using a 63 × 1.4 NA lens. To set the background fluorescence, the gain and slope settings for the photomultipliers were adjusted using cells treated with normal rabbit serum followed by secondary antibody. In the colocalization analysis, a yellow pixel represents equal intensities from the red and green channel.

RESULTS

Synchronization of IIC9 Cells in G_0—IIC9 fibroblasts were arrested in G_0 by serum starvation for 48 h. The incorporation of [^{3}H]thymidine into DNA was negligible in the serum-starved cells (Fig. 1*A*). The addition of 10% serum resulted in a wave of [^{3}H]thymidine incorporation beginning ~14 h poststimulation, peaking at ~22 h, and declining thereafter. Since at the peak (22 h) the thymidine incorporation rate was ~3 times that of nonsynchronized cells at the onset of serum starvation, this suggests that 3 times as many cells were in S phase. S phase typically occupies 30–40% of the cell cycle time. Thus, nearly all of the cells participated in the DNA synthesis wave, suggesting that they were synchronized initially in G_0.

To further assess the cell cycle status of the serum-starved cells, the level of cyclin D1 was examined by immunoblot analysis of cell lysates. The expression of cyclin D1 is low in G_0 cells, increases during the period of entry into G_1, and plummets during S phase (41). Serum-starved IIC9 cells had low but detectable levels of cyclin D1. This low expression level persisted at 2, 4, 6, and 8 h postserum, rose markedly between 8 and 10 h, and remained high until at least 24 h postserum (Fig. 1*B*).

The Rate of PC Synthesis Is Stimulated during Exit from G_0—The incorporation of [^{3}H]choline into PC during 10-min pulses was stimulated 3-fold as early as 10 min after the addition of serum compared with serum-starved cells (Fig. 1*C*).

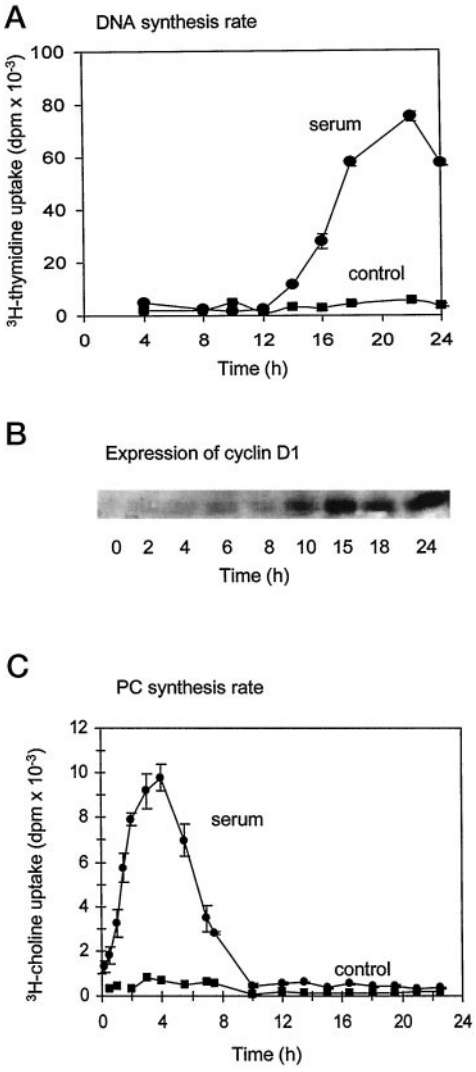

FIG. 1. **PC synthesis is stimulated during exit from G_0.** IIC9 cells were serum-starved for 48 h, followed by the addition of FBS to a final concentration of 10% (●) or continued incubation with the serum starvation medium (■). *A*, the incorporation of [^{3}H]thymidine into acid-insoluble material was measured at the indicated times (2-h pulses) as described under "Materials and Methods." The experiment was repeated twice with similar results. *B*, 50 μg of cell extracts were analyzed by Western blot with cyclin D1 antibody as described in materials and methods. The region of the gel corresponding to 32 kDa is shown. The experiment was repeated twice with similar results. *C*, the incorporation of [^{3}H]choline into a total lipid extract was measured at the indicated times (10-min pulses) as described under "Materials and Methods." The experiment was repeated five times with similar results. For *A* and *C*, data represent the average ± the error of duplicate determinations. Background dpm was assessed by methanol-treating cells prior to label incorporation, and this value was subtracted to yield the data shown.

A dramatic elevation in PC synthesis rates continued for 3–4 h, at which time there was an 11 ± 3-fold (n = 6) increase over control rates. The rate of PC synthesis declined to near basal levels between 4 and 10 h postserum. The return to basal PC synthesis rates probably coincides with the G_0/G_1 boundary (42).

To determine whether the burst in the PC synthesis rate resulted in accumulation of PC, we quantified the mass of PC in cells following stimulation by serum. In two independent determinations, the PC content of quiescent cells was 23 ± 2 nmol of PC/10^6 cells. The PC content at 4 and 7 h postserum was 26 ± 3 and 24 ± 3 nmol of PC/10^6 cells, respectively. Thus, the synthesis wave was accompanied by a nearly equivalent wave

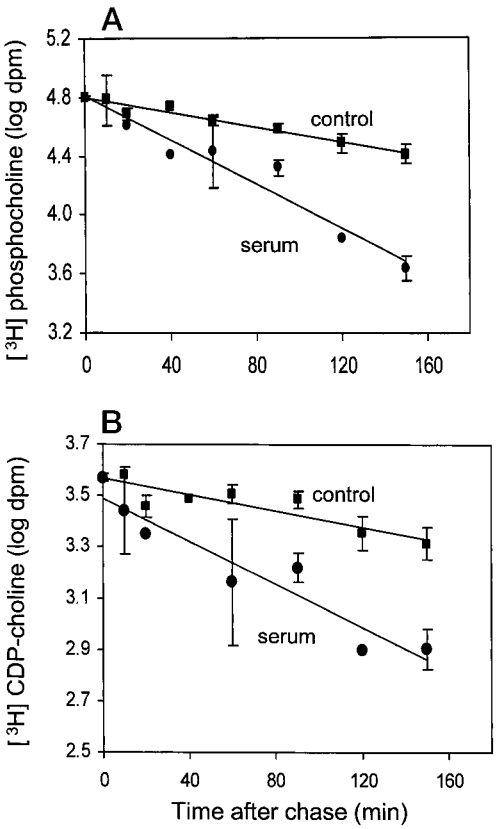

FIG. 2. **Phosphocholine and CDP-choline turnover are stimulated during exit from G_0.** IIC9 cells were serum-starved for 48 h and were labeled during the last hour with 2 μCi/ml [^{3}H]choline/60-mm dish. Cultures were chased with unlabeled medium containing 10% FBS (●) or unsupplemented (■). At the indicated times after chase, extracts were prepared, and the radioactivity in phosphocholine (*A*) and CDP-choline (*B*) was measured as described under "Materials and Methods." The experiment was repeated with similar results.

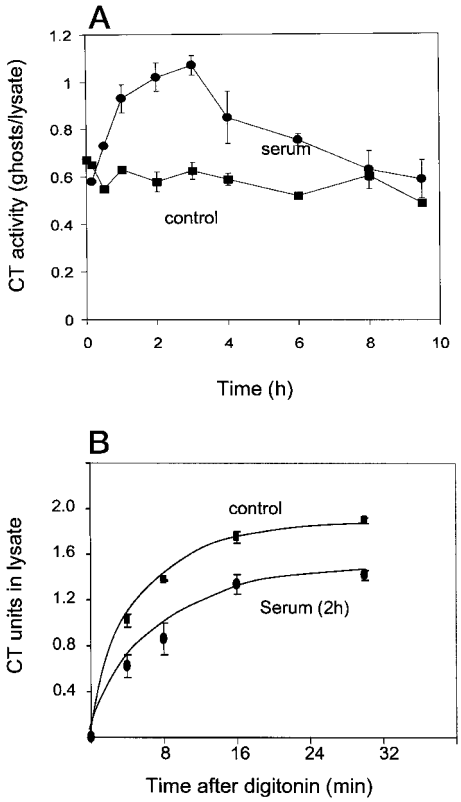

FIG. 3. **The ratio of membrane-bound: soluble CT increases during exit from G_0.** *A*, at the indicated times after the addition of FBS to a final concentration of 10% (●) or continued incubation with the serum starvation medium (■), duplicate 100-mm dishes were digitonin-permeabilized for 30 min at 3 °C. CT activity was measured in the digitonin lysate and ghost fractions. Data represent the averages of three independent experiments. *B*, time course of digitonin release of CT after 2-h incubation with 10% FBS (●) or serum-starved control (■). Data represent averages ± error of two independent experiments. The total CT activity in ghost plus lysate fractions was 2.8 ± 0.2 units.

of PC degradation, as has been observed previously, for example in macrophages re-entering the cell cycle in response to CSF1 (2).

Phosphocholine Turnover Is Stimulated during Exit from G_0—The stimulation of the rate of [^{3}H]choline incorporation into PC was not due to an acceleration of choline transport. Uptake of [^{3}H]choline into the cells, monitored by 5-min pulses, was not significantly different for serum-starved and serum-stimulated cultures. The uptake rates were constant over a 4-h time course in both serum-starved and serum-stimulated cultures (not shown). The increase in choline incorporation into PC could be due to acceleration of the reactions catalyzed by choline kinase, cytidylyltransferase, cholinephosphotransferase (CPT), or a combination of these. The specific radioactivity of the pools of choline, phosphocholine, and CDP-choline reached equilibrium within 1 h of labeling with 2–3 μCi/ml [^{3}H]choline (28 μM), and the relative pool sizes in serum-starved cells were as follows: choline, 3 ± 2%; phosphocholine, 83 ± 4%; and CDP-choline, 14 ± 2% (n = 3). These ratios suggest a rate-limiting step at the conversion of phosphocholine into CDP-choline, catalyzed by CT. The relative pool sizes were altered in cells treated with serum for 2–3 h: choline, 1%; phosphocholine, 73 ± 1%; and CDP-choline, 26.4 ± 0.6%. The phosphocholine:CDP-choline ratio decreased >2-fold, indicative of an acceleration of the CT-catalyzed step. The flux of [^{3}H]choline through the CDP-choline pathway was monitored by a pulse-chase regime (43). The label associated with intracellular choline completely turned over within 20 min after the onset of the cold chase in both control and serum-stimulated cultures. The turnover of phosphocholine and CDP-choline is shown in Fig. 2. The turnover times determined from these plots reflect the rates of the CT and CPT reactions *in situ*. The $t_{1/2}$ values for both phosphocholine and CDP-choline were reduced ~3-fold in the serum-stimulated cells (Fig. 2, *A* and *B*). These data suggest that the stimulation of PC synthesis during exit from G_0 is accompanied by acceleration of the CT and CPT reactions. We further examined the regulation of CT by serum.

The Affinity of CT for Organelles Increases during Exit from G_0—The serum-stimulated increase in the CT reaction was not due to an increase in the levels of the enzyme in the cell. Endogenous CT was immunoprecipitated from the IIC9 cell homogenates over the time course and detected by Western blot (Fig. 7*A*). There was no change in CT mass up to 8.5 h after serum stimulation. CT activity was also examined in cell homogenates from serum-starved and stimulated cells under optimal substrate and lipid activator concentrations. No significant effects of serum on the CT activity were observed (data not shown). Thus, the increase in CT activity measured *in situ* (Fig. 3) in response to serum may be a result of a post-translational activation mechanism that is not preserved in a cell-free extract.

One well described mechanism for the regulation of CT is its activating interaction with membrane lipids (10, 44, 45). We examined whether the observed increase in CT activity correlated with an increase in the affinity of CT for cell membranes using digitonin permeabilization (Fig. 3). Digitonin permeabilization of cells results in release of soluble proteins, while

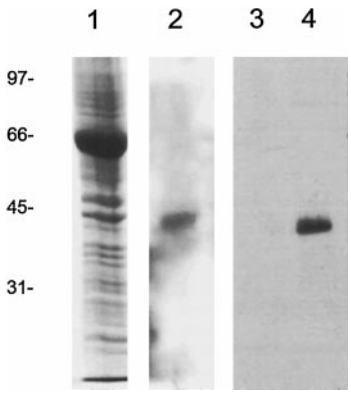

FIG. 4. **Specificity of domain M antibody for CT.** *Lane 1*, Coomassie stain of 20 μg of homogenate from IIC9 cells; *lane 2*, Western blot of 50 μg of IIC9 homogenate with a 1:1000 dilution of anti-M; *lane 3*, immunoprecipitation of lysate from [^{35}S]methionine and cysteine-labeled IIC9 cells with preimmune serum; *lane 4*, immunoprecipitation of cells as in *lane 3* with anti-M. See "Materials and Methods" for details.

organelle-trapped, cytoskeletal, and membrane-bound proteins remain in the cell ghosts. Oleic acid is a well documented promoter of CT membrane association (46–49). Control experiments, in which IIC9 cells were incubated with 0.1–1 mM oleic acid before permeabilization with 0.2 mg/ml digitonin, resulted in a concentration-dependent accumulation of CT in the ghost fraction (from 28% in untreated cells to 100% in 1 mM oleic acid-treated cells), as has been observed previously with other cells (50). When serum was added for 2 h prior to digitonin permeabilization, both the rate and the amount of CT released from cells decreased (Fig. 3*B*). We interpret this change as an increase in the membrane affinity of CT (see "Discussion"). Cells were treated with or without serum for 0–9.5 h followed by digitonin permeabilization for 30 min, and the fractions were analyzed for CT activity. The ratio of CT in the ghost *versus* lysate fractions is plotted in Fig. 3*A*. Serum stimulation generated an increase in the ratio of particulate/soluble CT, which was apparent within 30 min, peaked at 3 h, and declined to basal values within 8 h. Thus, the pattern of change in CT organelle affinity resembles the pattern of change in PC synthesis rates (Fig. 1*C*).

Confocal Imaging of CT's Intracellular Localization during Exit from G_0—We examined the intracellular distribution of CT during exit from G_0 by laser scanning confocal microscopy. To do this work, it was vital to use an antibody having high specificity for the enzyme. An antipeptide antibody against residues 256–288 of rat liver CT (anti-M) reacted selectively with the 42-kDa CT band in a Western blot of crude lysate from IIC9 cells (Fig. 4, *lane 2*). In addition, a 42-kDa protein from [^{35}S]methionine-labeled cells was specifically immunoprecipitated by this antibody (Fig. 4, *lane 4*).

Fig. 5*A* shows images of fixed IIC9 cells from nonsynchronized, serum-starved, and serum-stimulated cultures. Nonsynchronized cultures showed heterogeneity from cell to cell in CT distribution. CT was primarily nuclear in most of the cells but was cytoplasmic or distributed in both compartments in the rest of the population. In quiescent cells, CT was localized almost exclusively in the nucleus and had a punctate distribution there. Within 10 min postserum, CT was clearly visible in the cytoplasm of most cells. The cytoplasmic fluorescence continued to increase, while the nuclear intensity decreased (but did not disappear) up to 4 h postserum. The cytoplasmic fluorescence was also punctate and was concentrated in the perinuclear region. After 4 h, the trend reversed as the ratio of nuclear/cytoplasmic fluorescence increased. By 8 h, CT was again predominantly nuclear. The time course of redistribution of CT from the nucleus into the cytoplasm and back into the nucleus paralleled the wave of PC synthesis (Fig. 1*C*) and the changes in CT-membrane affinity (Fig. 3*A*).

Although almost all of the cellular CT from quiescent cells and from cells 8 h postserum was nuclear (Fig. 5*A*), digitonin treatment (200 μg/ml) released ~65% of the CT (Fig. 3). These data appear to be contradictory, unless the digitonin were permeabilizing the nuclear membranes. Watkins and Kent (51) previously showed that the nuclear staining of CT was lost upon treatment of Chinese hamster ovary cells with 0.8 mg/ml digitonin. Digitonin (200 μg/ml) also released ~90% of cyclin D1 (data not shown), which is confined to the nucleus 12 h postserum (41). There was minimal release of CT (12 ± 3%) and cyclin D1 (16 ± 0.3%) from cells treated with 40 μg/ml digitonin (data not shown), a concentration used in reconstitution of nuclear import to permeabilize plasma membranes without disruption of the nuclear membrane (52–54). These data suggest that 200 μg/ml digitonin permeabilizes the nuclear membrane.

Recently, a CT isoform (CT-β) was identified in many tissues that is missing the nuclear localization signal and is found exclusively in the cytoplasm (55). We therefore examined the intracellular distribution of CT-β in serum-starved and serum-stimulated IIC9 cells, using an antibody specific for the divergent N terminus of CT-β. When the fluorescence distributions of anti-M *versus* anti-CT-β were compared using cells treated in parallel, we found notable differences (Fig. 5*B*). In quiescent cells, while the anti-M signal was confined to the nucleus, the anti CT-β signal was cytoplasmic. The very low cytoplasmic fluorescence in G_0 cells detected using anti-M (directed against a CT-α peptide whose sequence is 85% identical to that segment in CT-β) may be due to a relatively low abundance of CT-β *versus* CT-α and/or a greater affinity between anti-M and CT-α. CT-β fluorescence pattern 2 h postserum stimulation did not change, unlike the anti-M signal, which redistributed from the nucleus to the cytoplasm. These data suggest that the localization changes induced by serum are associated with CT-α, not CT-β.

To identify the cytoplasmic structure with which CT interacts during exit from G_0, we examined the co-localization of CT in serum-stimulated cells with various organelle markers, beginning with an ER marker. Fig. 5*C* shows a double indirect labeling of a group of cells with the anti-CT antibody (anti-M) and an antibody directed against BiP, a resident of the ER lumen. This group of four cells is representative of the field from a culture 1 h postserum. These images show reticular distribution of BiP that is more intense in the perinuclear region and a similar albeit more punctate distribution of CT in the cytoplasm. The pattern is consistent with co-localization of the majority of cytoplasmic CT with the ER and was evident whether the CT or the BiP antibody was added first. Co-localization of the two fluorophores was very strong in the perinuclear region. This pattern was also observed when cells were co-labeled with the CT antibody and the direct ER marker, rhodamine hexyl ester (data not shown).

The specificity of the CT-ER co-localization was probed by comparison of CT distribution with that of F-actin, directly labeled with rhodamine phalloidin, and mitochondria, directly labeled with a vital stain. Whereas CT distribution was punctate in the nucleus and cytoplasm, the distribution of F-actin was fibrillar, and the pattern of the mitochondrial stain was also distinct from that of cytoplasmic CT (data not shown).

Phosphorylation State of CT during the G_0 to G_1 Transition—Analysis of CT phosphorylation mutants and the effects of phosphatase inhibitors suggests that the phosphorylation state of CT participates in the regulation of the membrane affinity

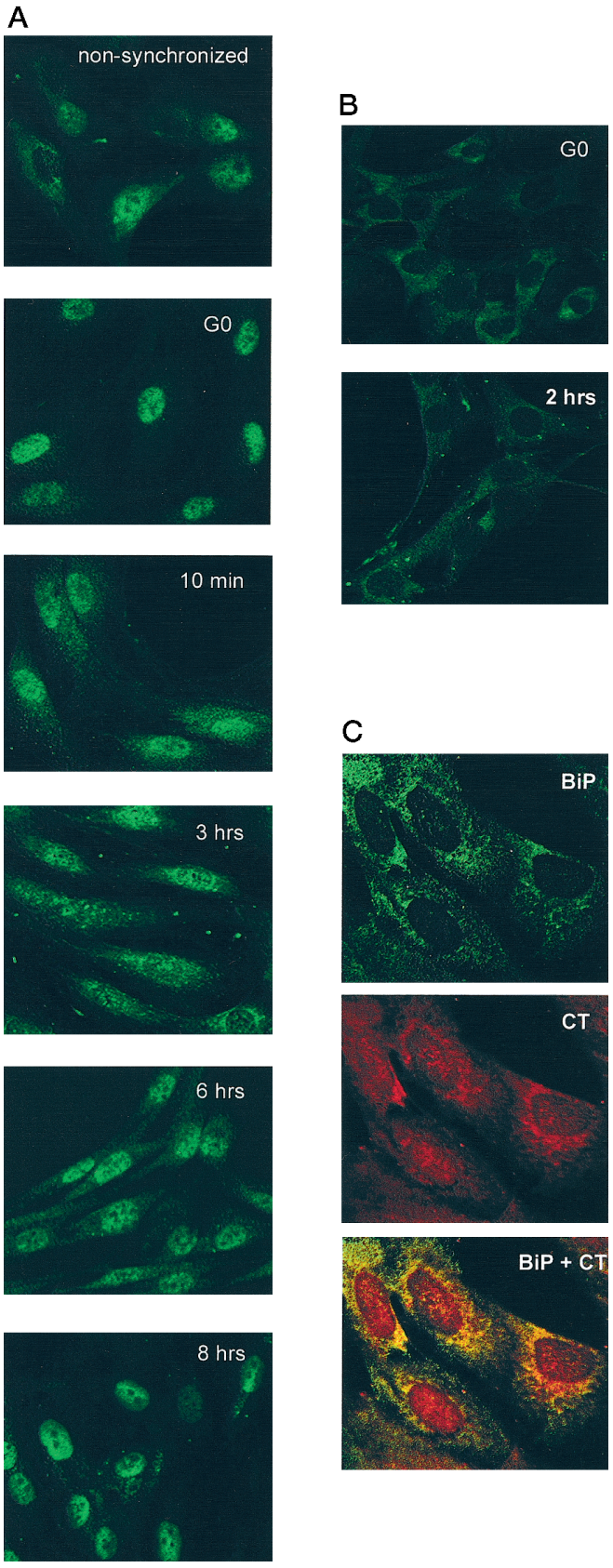

FIG. 5. **Intracellular redistribution of CT during exit from G_0.** *A*, fluorescence labeling of CT-α; IIC9 cells were grown on coverslips and were serum-starved for 48 h. At the indicated times after the addition of FBS to a final concentration of 10%, coverslips were fixed and labeled with anti-M followed by labeling with a GAR Oregon Green-conjugated secondary antibody as described under "Materials and Methods." Optical sections were obtained by confocal microscopy of representative fields. These images represent the pattern of localization found in six independent experiments, where a total of 750 cells were scored for nuclear *versus* cytoplasmic fluorescence. The times indicate the duration of serum treatment prior to fixation. *B*, fluorescence labeling of CT-β; IIC9 cells were treated as described for *A*, except the primary antibody was to CT-β. Images represent the pattern of localization found in three independent experiments. When images were captured using identical confocal parameters as in *A*, staining of CT-β was barely visible; therefore, both the brightness and contrast were enhanced in Adobe Photoshop. *C*, double labeling of CT and BiP in IIC9 cells. At 1 h following the addition of serum to a final concentration of 10%, coverslips were fixed and labeled in the following order: rabbit polyclonal anti-M (directed against CT), Texas Red GAR, mouse monoclonal anti-BiP, Oregon Green GAM. Data from the red and green channels are shown separately before manual overlay in Adobe Photoshop. *Red* represents CT, *green* represents BiP, and *yellow* represents co-localization of CT and BiP.

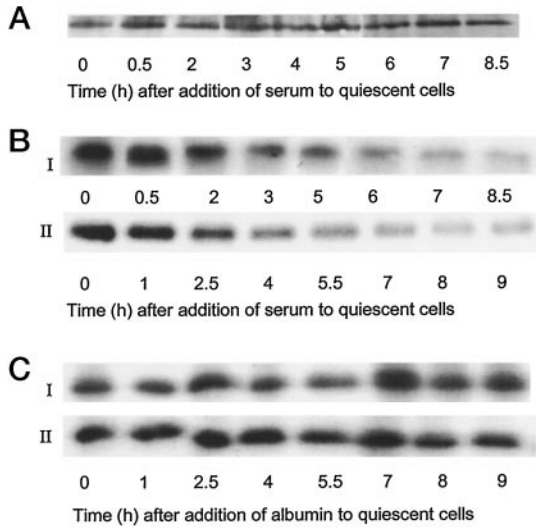

FIG. 6. **CT mass and phosphorylation state during exit from G_0.** *A*, Western blot. At the indicated times after the addition of 10% FBS to serum-starved cells, cell extracts were prepared, and CT was immunoprecipitated and analyzed by SDS-polyacrylamide gel electrophoresis and Western blot as described under "Materials and Methods." Each lane represents an immunoprecipitate from one 150-mm dish. The experiment was repeated twice, showing a pattern of constant CT mass over 8 h. *B* and *C*, autoradiogram. 32 h after serum starvation, the medium was replaced with phosphate-free DMEM containing 0.1 mCi/ml [^{32}P]orthophosphate. After an additional 16-h incubation, FBS (10%) (*B*) or BSA (5%) (*C*) was added. At the indicated times, cell extracts were prepared, and CT was immunoprecipitated. The amount of ^{32}P label associated with CT was determined by SDS-polyacrylamide gel electrophoresis and autoradiography. Each lane represents an immunoprecipitate from one 150-mm dish. The experiments shown in *B* were performed six times with similar results. Two separate experiments are shown in *B* and *C* (*I* and *II*).

and activity of the enzyme (12–14, 56, 57). Moreover, the phosphorylation status of CT fluctuated during G_1 in concert with its activity, measured *in vitro* (2). We labeled quiescent IIC9 cells with [^{32}P]orthophosphate, added serum for various time periods, and immunoprecipitated CT. There was no decrease in ^{32}P label associated with the CT band at 1 h after the addition of serum, but beginning at ~2 h postserum, the intensity of the label progressively decreased to minimal amounts by 8 h (Fig. 6*B*). By comparison, the ^{32}P signal associated with CT immunoprecipitated from cultures receiving 5% albumin rather than serum did not change over this time (Fig. 6*C*). In a separate experiment, ^{32}P-labeled, immunoprecipitated CT was detected by immunoblot and then autoradiographed to assess the ^{32}P label intensity. A comparison of the signals from the film and the blot confirmed that the ^{32}P label, but not the mass of CT, was decreasing during the G_0 to G_1 transition (data not shown). The kinetics of the changes in CT phosphorylation did not coincide with the changes in CT activity (Fig. 2*A*), translocation

to cell membranes (Fig. 3*A*), or the wave of PC synthesis (Fig. 1*C*). Dephosphorylation of CT was subsequent to the other stimulatory effects on the enzyme, and the return to basal activity and membrane affinity occurred without rephosphorylation of the enzyme.

DISCUSSION

The data in this paper suggest a novel regulatory mechanism for membrane phospholipid synthesis during entry into the cell cycle. We have unraveled a tight kinetic coupling between the regulation of PC synthesis, the activity and membrane affinity of the regulatory enzyme, CT, and its distribution between the nucleus and ER. This coupling leads to the proposal that the nucleus serves as a repository for inactive (or less active) CT and that signals promoting PC metabolism operate via translocation of the enzyme to its functional site on the ER. The nuclear localization of CT has been a puzzle ever since that discovery over 10 years ago (22). In the intervening time, other enzymes of lipid metabolism, such as phospholipase C, D, and A_2 isoforms, 5-lipoxygenase, various PI kinases, and DAG kinase have been detected in the nucleus, giving rise to the notion of nuclear lipid signaling pathways (58). Regulated redistribution of DAG kinase ζ (59) and 5-lipoxygenase (60) between the nucleus and cytoplasm has been reported. DAG kinase translocation out of the nucleus, driven by protein kinase C-mediated phosphorylation, serves to isolate the enzyme from its nuclear DAG substrate, thereby prolonging the activation of protein kinase C (59). Translocation of 5-lipoxygenase to the nucleus of neutrophils is stimulated by cell adherence, but this event does not result in an activation of leukotriene synthesis (60). Unlike these enzymes, the expulsion of CT from the nucleus appears to be linked to its activation.

A Wave of PC Synthesis and CT Activation Accompanies Exit from G_0 in Response to PC Degradation—Our results show a ~10-fold surge in the rate of PC synthesis during re-entry into the cell cycle that did not translate into a large accumulation of PC. The most likely explanation is that serum growth factors stimulate both PC synthesis and hydrolysis (1, 2). The hydrolysis is to generate lipid second messengers, and the synthesis is probably a response to maintain PC homeostasis (61). It has been estimated that 75% of the PC turns over during the cell cycle re-entry period (1, 2). These data are in agreement with other evidence suggesting that the re-entry phase is not accompanied by an increase in cell mass and volume (42). The doubling of PC mass needed for cell division occurs during S phase as a consequence of drastically reduced PC degradation rates (1, 2). In keeping with this observation, PC mass in IIC9 cells increased by 60% at 25 h postserum, and 80% at 27 h postserum, *i.e.* near the S/G_2 boundary (data not shown).

The effect of serum on choline flux during the first 2.5 h revealed a ~3-fold acceleration of the CT- and CPT-catalyzed steps, based on turnover $t_{1/2}$. The accelerated flux led to the biggest changes in the phosphocholine pool size, which decreased 3-fold at 2 h and 4-fold at 3 h postserum, compared with serum-starved controls. The CDP-choline pool decreased ~40% by 3 h postserum. We were unable to define the effects of serum on intracellular choline turnover because the choline pool was so small and turned over so rapidly in the IIC9 cells. In 3T3 cells, the choline kinase reaction was stimulated by serum, leading to swelling of the phosphocholine pool (28). This was not observed in the IIC9 cells, and none of our [^{3}H]choline flux analyses indicated a regulation at the choline kinase step. The pool size analysis indicated that the CT-catalyzed step is rate-limiting and that serum generated the largest depletion of phosphocholine, the substrate for CT. Thus, it is likely that the CT reaction is the primary step regulated by the serum growth factors and that the CPT-catalyzed step accelerates in response to increased supply of CDP-choline. There is precedence for control of CPT by substrate supply in cells (39, 62).

What stimulates CT during exit from G_0 in IIC9 cells is unknown. The increased activity is not due to increased enzyme expression (Fig. 6*A*). This finding is in agreement with the effects upon stimulation of cell cycling of BAC1.2F5 cells with CSF-1. Although CSF-1 induced a 4-fold elevation of CT mRNA (16), the wave of CT mRNA did not correlate kinetically with the wave of CT activity, which was similar to the kinetics of PC synthesis that we observed (2). Two factors were clearly identified in this study that correlate kinetically with changes in CT activity: (i) CT's membrane affinity and (ii) CT's relocalization between nucleus and ER.

Changes in CT Membrane Affinity Parallel the Wave of PC Synthesis Accompanying the Exit from G_0—CT has been characterized as an amphitrophic enzyme, *i.e.* it has two intracellular localizations. Many conditions that stimulate PC synthesis are associated with a translocation of CT from the soluble to the particulate fraction (8, 9, 44, 61). In our analyses of CT distribution in IIC9 cells, the distribution of CT between soluble and particulate phases depended on the volume of the digitonin buffer and the digitonin concentration. Nevertheless, when the permeabilization conditions are carefully calibrated, the method provides useful comparative data. For the data in Fig. 3, permeabilization conditions were such that 63 ± 3% of the CT was in the digitonin lysate in the control cells compared with 48 ± 1.5% in cells serum-stimulated for 3 h. When digitonin permeabilization conditions were set so that 90% of the CT appeared in the lysate in the controls, we still observed an increase in the ratio of ghost/lysate CT upon serum stimulation between 1 and 4 h and a decline to near basal values by 10 h postserum. The changes in CT distribution were slightly in advance of the PC synthesis wave (compare Figs. 1*C* and 3*A*), which is in accord with the notion that changes in CT membrane affinity control PC synthesis. The reduction in the fraction of CT released by digitonin could be brought on by factors other than an increase in the enzyme's membrane affinity. However, this interpretation of the data is supported by other data: (i) lipids such as fatty acids or diacylglycerol, which increase the affinity of CT for lipid vesicles, also reduce the fraction of cellular CT released by digitonin (63); (ii) CT's redistribution to the ER during exit from G_0 accompanies the reduction in digitonin-releasable CT.

Relocalization of CT from the Nucleus to the ER Accompanies the Wave of PC Synthesis during Exit from G_0—Previous data reveal CT in the nucleus (19) in both nuclear and cytoplasmic compartments or mainly in the cytoplasm (20), depending on cell type as well as the method of localization. Our data suggest that the localization of CT (specifically, CT-α) is dynamic and depends, for one thing, on the phase of the cell cycle. In the previous CT localization studies, the cell cycle phase was not examined.

Phospholipase C treatment of Chinese hamster ovary cells led to a stimulation of PC synthesis (61) and translocation of CT from nucleoplasm to the nuclear envelope (51). The nuclear envelope localization, detected by indirect immunofluorescence was distinct from the pattern of an ER marker (51). A similar redistribution between the nucleus and nuclear envelope was observed in HeLa cells following stimulation with oleic acid (49). These results differ from our observations showing that translocation to the ER accompanies CT activation. The systems for stimulating PC synthesis differ among these studies. The addition of high concentrations of oleic acid or phospholipase C to the culture medium probably leads to elevated concentrations of oleic acid or DAG in *all* cell membranes, including the nuclear membranes. Since these lipids will di-

rectly induce translocation, the simplest mechanism would be for CT to bind to the membrane of nearest proximity, the inner nuclear membrane. In the system we have explored, re-entry into the cell cycle, it may be that the signals that enhance CT binding to membranes are produced selectively in the ER, hence the translocation to that site alone.

CT-α has a nuclear localization signal at its N terminus that drives its import (24). The existence of a signal for regulated export from the nucleus such as the leucine-rich motif identified in a handful of proteins (64–66) has not been explored. Attempts to block CT-α's nuclear export using leptomycin B, a specific inhibitor of exportin 1-dependent nuclear export (67), were negative. Thus, the exit of CT from the nucleus is unlikely to be due to the presence of a leucine-rich nuclear export signal. The strength of the nuclear *versus* cytoplasmic localizing forces on CT-α may depend on the presence of growth factor-dependent signal(s) in the ER membrane, which would increase the lifetime of CT-α bound to the ER.

Model of CT Regulation during Exit from G_0—The results of this study present the following model for CT-α regulation during the G_0 to G_1 transition. In G_0, CT-α is localized in the nucleus, is highly phosphorylated, and is relatively inactive with respect to PC synthesis. Growth factors that trigger progression into the cell cycle induce the relocalization of most of the nuclear CT-α to the cytoplasm, where it binds to the cytoplasmic face of the ER. Based on the digitonin permeabilization data, the binding to the ER is of higher affinity than the binding to nuclear structures. Activation of CT *in vitro* requires insertion of an amphipathic helix into the lipid core of a membrane (10, 15, 36). The ER localization means that the product of the CT reaction, CDP-choline, will be localized near the next enzyme in the pathway, CPT, an integral membrane protein of the ER, whose active site faces the cytoplasm (68). This, combined with an increase in the rate of production of CDP-choline due to CT activation on the ER, results in a burst of PC synthesis. Approximately 4 h postserum, CT-α's affinity for the ER weakens, and it returns to the nucleus, coincident with a decline in PC synthesis. These data offer a hypothesis for the role of nuclear localization of CT-α. It is a holding bin for CT when the demand for PC synthesis is low. Signals that increase demand for PC synthesis recruit CT-α from the holding bin to its functional site, the ER. On the other hand, CT-α may have a function in addition to catalyzing the formation of CDP-choline, which operates in the nucleus, and this function could be related to cell cycle control.

The factors that induce the changes in CT activity, localization and membrane affinity during exit from G_0 are not known. One potential factor, the phosphorylation state of CT, does not drive the relocalization. Phosphorylation regulates the nuclear export of MAPKAP kinase-2 (69) and DAG kinase ζ (59). If changes in the net phosphorylation status of the enzyme were responsible for the activation of CT, then a decrease in phosphorylation should have been observed in less than 1 h, and an increase in phosphorylation should have been observed between 4 and 5 h, returning to the highly phosphorylated state by ~8 h. This is not the pattern obtained (see Fig. 6*B*). Our results are consistent with other studies showing that enzyme dephosphorylation is subsequent to membrane binding in response to phospholipase C and oleic acid (70). The potential role of specific phosphorylation sites on CT localization could be examined in the future using site-specific mutants. We hypothesize that products of PC catabolism, such as DAG, phosphatidic acid, or arachidonic acid, could be direct activators. These lipid mediators directly activate the purified enzyme *in vitro* and when their amounts are manipulated in cells (9). The involvement of these lipids in the regulation of CT during exit from G_0 is currently being investigated.

Acknowledgments—We are grateful for the contributions of Dr. Rebecca Arnold at the onset of this project and the contributions of Michael Ng. We thank Dr. Dan Raben for the gift of the IIC9 cells, Dr. Suzanne Jackowski for the gift of the CT-β antibody, Dr. John Aitchison for the gift of leptomycin B, and Dr. Dennis Vance for comments on the manuscript.

REFERENCES

1. Jackowski, S. (1996) *J. Biol. Chem.* **271,** 20219–20222
2. Jackowski, S. (1994) *J. Biol. Chem.* **269,** 3858–3867
3. Cornell, R., Grove, G. L., Rothblat, G. H., and Horwitz, A. F. (1977) *Exp. Cell Res.* **109,** 299–307
4. Terce, F., Brun, H., and Vance, D. E. (1994) *J Lipid Res.* **35,** 2130–2142
5. Cui, Z., Houweling, M., Chen, M. H., Record, M., Chap, H., Vance, D. E., and Terce, F. (1996) *J. Biol. Chem.* **271,** 14668–14671
6. Baburina, I., and Jackowski, S. (1998) *J. Biol. Chem.* **273,** 2169–2173
7. Miquel, K., Pradines, A., Terce, F., Selmi, S., and Favre, G. (1998) *J. Biol. Chem.* **273,** 26179–26186
8. Tronchere, H., Record, M., Terce, F., and Chap, H. (1994) *Biochim. Biophys. Acta* **1212,** 137–151
9. Cornell, R. B. (1996) in *Advances in Lipobiology* (Gross, R., ed) Vol. 1, pp. 1–38, JAI Press, London
10. Cornell, R. B. (1998) *Biochem. Soc. Trans.* **26,** 539–544
11. Kent, C. (1997) *Biochim. Biophys. Acta* **1348,** 79–90
12. Wang, Y., and Kent, C. (1995) *J. Biol. Chem.* **270,** 17843–17849
13. Yang, W., and Jackowski, S. (1995) *J. Biol. Chem.* **270,** 16503–16506
14. Arnold, R. S., DePaoli-Roach, A. A., and Cornell, R. B. (1997) *Biochemistry* **36,** 6149–6156
15. Arnold, R. S., and Cornell, R. B. (1996) *Biochemistry* **35,** 9917–9924
16. Tessner, T. G., Rock, C. O., Kalmar, G. B., Cornell, R. B., and Jackowski, S. (1991) *J. Biol. Chem.* **266,** 16261–16264
17. Houweling, M., Tijburg, L. B., Vaartjes, W. J., Batenburg, J. J., Kalmar, G. B., Cornell, R. B., and Van Golde, L. M. (1993) *Eur. J. Biochem.* **214,** 927–933
18. Hogan, M., Kuliszewski, M., Lee, W., and Post, M. (1996) *Biochem. J.* **314,** 799–803
19. Wang, Y., Sweitzer, T. D., Weinhold, P. A., and Kent, C. (1993) *J. Biol. Chem.* **268,** 5899–5904
20. Houweling, M., Cui, Z., Anfuso, C. D., Bussiere, M., Chen, M. H., and Vance, D. E. (1996) *Eur J. Cell Biol.* **69,** 55–63
21. Vance, J. E., and Vance, D. E. (1988) *J. Biol. Chem.* **263,** 5898–5909
22. Morand, J. N., and Kent, C. (1989) *J. Biol. Chem.* **264,** 13785–13792
23. Terce, F., Record, M., Tronchere, H., Ribbes, G., and Chap, H. (1991) *Biochim. Biophys. Acta* **1084,** 69–77
24. Wang, Y., MacDonald, J. I., and Kent, C. (1995) *J. Biol. Chem.* **270,** 354–360
25. Wright, T. M., Shin, H. S., and Raben, D. M. (1990) *Biochem. J.* **267,** 501–507
26. Exton, J. H. (1994) *Biochim. Biophys. Acta* **1212,** 26–42
27. Paddon, H. B., and Vance, D. E. (1980) *Biochim. Biophys. Acta* **620,** 636–640
28. Warden, C. H., and Friedkin, M. (1985) *J. Biol. Chem.* **260,** 6006–6011
29. Wieprecht, M., Wieder, T., Geilen, C. C., and Orfanos, C. E. (1994) *FEBS Lett.* **353,** 221–224
30. MacDonald, J. I., and Possmayer, F. (1995) *Biochem. J.* **312,** 425–431
31. Tran, K., Man, R. Y., and Choy, P. C. (1995) *Biochim. Biophys. Acta* **1259,** 283–290
32. Pelech, S. L., and Vance, D. E. (1989) *Trends Biochem. Sci.* **14,** 28–30
33. Morash, S. C., Rose, S. D., Byers, D. M., Ridgway, N. D., and Cook, H. W. (1998) *Biochem. J.* **332,** 321–327
34. Wright, T. M., Rangan, L. A., Shin, H. S., and Raben, D. M. (1988) *J. Biol. Chem.* **263,** 9374–9380
35. Wright, T. M., Willenberger, S., and Raben, D. M. (1992) *Biochem. J.* **285,** 395–400
36. Johnson, J. E., Aebersold, R., and Cornell, R. B. (1997) *Biochim. Biophys. Acta* **1324,** 273–284
37. Bligh, E. G., and Dyer, W. J. (1959) *Can. J. Biochem. Physiol.* **62,** 983–988
38. Bartlett, G. R. (1959) *J. Biol. Chem.* **234,** 466–468
39. Walkey, C. J., Kalmar, G. B., and Cornell, R. B. (1994) *J. Biol. Chem.* **269,** 5742–5749
40. Cornell, R. (1989) *J. Biol. Chem.* **264,** 9077–9082
41. Baldin, V., Lukas, J., Marcote, M. J., Pagano, M., and Draetta, G. (1993) *Genes Dev.* **7,** 812–821
42. Zetterberg, A. (1996) in *Apoptosis and Cell Cycle Control in Cancer* (Thomas, N. S. B., ed) pp. 17–35, Bios Scientific, Oxford
43. Vance, D. E., Trip, E. M., and Paddon, H. B. (1980) *J. Biol. Chem.* **255,** 1064–1069
44. Vance, D. E., and Pelech, S. L. (1984) *Trends Biochem. Sci.* **9,** 17–20
45. Bladergroen, B. A., Wensing, T., Van Golde, L. M., and Geelen, M. J. H. (1998) *Biochim. Biophys. Acta* **1391,** 233–240
46. Weinhold, P. A., Rounsifer, M. E., Williams, S. E., Brubaker, P. G., and Feldman, D. A. (1984) *J. Biol. Chem.* **259,** 10315–10321
47. Cornell, R., and Vance, D. E. (1987) *Biochim. Biophys. Acta* **919,** 26–36
48. Pelech, S. L., Pritchard, P. H., Brindley, D. N., and Vance, D. E. (1983) *J. Biol. Chem.* **258,** 6782–6788
49. Wang, Y., MacDonald, J. I., and Kent, C. (1993) *J. Biol. Chem.* **268,** 5512–5518
50. Weinhold, P. A., and Barrett, D. (1998) *Biochim. Biophys. Acta* **1391,** 307–319
51. Watkins, J. D., and Kent, C. (1992) *J. Biol. Chem.* **267,** 5686–5692
52. Cserpan, I., and Udvardy, A. (1995) *J. Cell Sci.* **108,** 1849–1861
53. Kehlenbach, R. H., Dickmanns, A., and Gerace, L. (1998) *J. Cell Biol.* **141,** 863–874
54. Love, D. C., Sweitzer, T. D., and Hanover, J. A. (1998) *Proc. Natl. Acad. Sci.*

U. S. A. **95,** 10608–10613
55. Lykidis, A., Murti, K. G., and Jackowski, S. (1998) *J. Biol. Chem.* **273,** 14022–14029
56. Watkins, J. D., and Kent, C. (1991) *J. Biol. Chem.* **266,** 21113–21117
57. Hatch, G. M., Jamil, H., Utal, A. K., and Vance, D. E. (1992) *J. Biol. Chem.* **267,** 15751–15758
58. D'Santos, C. S., Clarke, J. H., and Divecha, N. (1998) *Biochim. Biophys. Acta* **1436,** 201–232
59. Topham, M. K., Bunting, M., Zimmerman, G. A., McIntyre, T. M., Blackshear, P. J., and Prescott, S. M. (1998) *Nature* **394,** 697–700
60. Brock, T. G., McNish, R. W., Bailie, M. B., and Peters-Golden, M. (1997) *J. Biol. Chem.* **272,** 8276–8280
61. Sleight, R., and Kent, C. (1983) *J. Biol. Chem.* **258,** 831–835
62. Lim, P., Cornell, R., and Vance, D. E. (1986) *Biochem. Cell Biol.* **64,** 692–698
63. Cornell, R., and Vance, D. E. (1987) *Biochim. Biophys. Acta* **919,** 37–48
64. Wada, A., Fukuda, M., Mishima, M., and Nishida, E. (1998) *EMBO J.* **17,** 1635–1641
65. Toyoshima, F., Moriguchi, T., Wada, A., Fukuda, M., and Nishida, E. (1998) *EMBO J.* **17,** 2728–2735
66. Taagepera, S., McDonald, D., Loeb, J. E., Whitaker, L. L., McElroy, A. K., Wang, J. Y., and Hope, T. J. (1998) *Proc. Natl. Acad. Sci. U. S. A.* **95,** 7457–7462
67. Fornerod, M., Ohno, M., Yoshida, M., and Mattaj, I. W. (1997) *Cell* **90,** 1051–1060
68. Ballas, L. M., and Bell, R. M. (1980) *Biochim. Biophys. Acta* **602,** 578–590
69. Ben-Levy, R., Hooper, S., Wilson, R., Paterson, H. F., and Marshall, C. J. (1998) *Curr. Biol.* **8,** 1049–1057
70. Houweling, M., Jamil, H., Hatch, G. M., and Vance, D. E. (1994) *J. Biol. Chem.* **269,** 7544–7551

Shuttling of CTP:Phosphocholine Cytidylyltransferase between the Nucleus and Endoplasmic Reticulum Accompanies the Wave of Phosphatidylcholine Synthesis during the $G_0 \rightarrow G_1$ Transition

Ingrid C. Northwood, Amy H. Y. Tong, Bryan Crawford, Adrienne E. Drobnies and Rosemary B. Cornell

J. Biol. Chem. 1999, 274:26240-26248.
doi: 10.1074/jbc.274.37.26240

Shuttling of CTP:Phosphocholine cytidylyltransferase between the nucleus and endoplasmic reticulum accompanies the wave of phosphatidylcholine synthesis during the G(0) --> G(1) transition.

Northwood, Ingrid, C.; Tong, Amy, H. Y.; Crawford, Bryan, D.; Drobnies, Adrienne, E.; Cornell, Rosemary, B.

1999

https://unbscholar.lib.unb.ca/handle/1882/22443